A Proposed Obstacle Sensor for a Mars Rover

WILLIAM L. KURIGER*
University of Oklahoma, Norman, Okla.

The unmanned surface vehicle planned for the exploration of Mars will require obstacle detection in order to navigate without direct human control. An injection laser rangefinder is proposed and analyzed for an obstacle detection sensor. Several different types of photodetectors are considered; the best signal-to-noise ratio is achieved with an avalanche photodiode. The proposed sensor scans the terrain without use of wearing parts by employing a vibrating mirror for elevation scan and a fixed array for azimuthal scan. Methods of processing the range data to discern the presence of obstacles are discussed, and an analog processing scheme is suggested.

Nomenclature

A_r = receiver antenna area = 0.49×10^{-3} m^2
A_v = voltage gain of postdetector amplifier
B = optical bandwidth = 50 Å
c = velocity of light = 3×10^8 m/sec
e = electronic charge = 1.602×10^{-19} coulombs
Δf = postdetection bandwidth = 250 MHz
F = noise factor of postdetection amplifier = 2
G = internal gain of photodetector = 1 for PIN diode, 5×10^4 for photomultiplier, 20, 100, or 200 for avalanche photodiode
h = Planck's const = 6.625×10^{-34} joule-sec
I_{av} = mean value of photocathode current
I_d = photodetector dark current (at cathode) = 0.15 nA for PIN diode, 3.25×10^{-16} A for photomultiplier, $10^{-8}/GA$ for avalanche photodiode
k = Boltzmann's const = 1.38×10^{-23} joules/°K
L = ground range
m = exponent of internal gain for noise power = 2 for photomultiplier, 2.3 for avalanche photodiode
M = solar spectral irradiance at 0.9 μm = 0.04 w/m² — Å
P_b = background power incident on detector photocathode
P_r = signal power incident on detector
P_t = laser power output (peak) = 13 w
Q,Q_s,Q_n = quantum efficiency, photoelectrons/photon = 0.5 for PIN diode, 3×10^{-3} for photomultiplier; Q_s = 0.3, Q_n = 0.9 for avalanche photodiode
R = range
R_L = photodetector load resistance = 50 ohms
T = absolute temperature = 290°K
T_a = Martian atmospheric transmission at 0.9 μm = 1
V_{sig} = signal voltage at output of post-detection amplifier
V_n = noise voltage at output of post-detection amplifier
α_v = receiver antenna vertical beamwidth = 3 milliradians
α_r = receiver antenna azimuthal beamwidth = 0.4 rad
Γ_r = efficiency of receiver optics = 0.5
Γ_t = efficiency of transmitter optics = 0.8
ξ = Martian surface reflectivity at 0.9 μm = 0.3
Φ = angle between direction of sun and surface normal
λ = operating wavelength = 0.902 μm

Introduction

THE exploration of Mars is expected to require the use of an unmanned surface roving vehicle. Because of the large and variable time delay involved in Earth-Mars communications, such a vehicle would be required to traverse the Martian surface with minimal external control; specifically, the vehicle should be able to detect obstacles and avoid them by making small deviations from an otherwise preplanned trajectory. It is the purpose of this paper to analyze the requirements for an obstacle detection system and propose a specific configuration for such a sensor.

The surface of Mars has not yet been observed with anywhere near the resolution necessary to distinguish objects on the scale of meters, thus possible distributions of obstacles are speculative. An extensive amount of work has been done with regard to probable obstacle distributions.[1] At present, it appears that with the possible exception of the chaotic terrain, the Martian surface will be sufficiently smooth that a roving vehicle will only occasionally encounter an obstacle. The Martian atmosphere is too tenuous to be a significant factor in the obstacle sensor design.

Moore[2] has performed a preliminary analysis of requirements for a Martian surface navigation capability. He envisions a vehicle equipped with both a short-range obstacle detector, to serve a purely protective function, and a relatively long-range obstacle detector which would permit the vehicle to sense obstacles such as boulders, small craters, and steep slopes in time to change its heading and so avoid them. Only the second function is considered in this paper.

Present plans are that the exploratory vehicle will be of six-wheeled articulated construction and will traverse the Martian surface at a typical rate of 0.5 km/hr, with a maximum speed of perhaps 1.5 km/hr. The obstacle detection sensor should mount directly on the vehicle and be capable of detecting obstacles with dimensions as small as 0.5 m. Design constraints include that the sensor should be capable of operating in bright sunlight, weigh no more than 10 lb, contain no moving parts, and consume at most 10 w of power.

Since the identification of obstacles is greatly facilitated if range information is known, the only form of obstacle detector considered is a rangefinder. Such a device using electromagnetic radiation in the infrared-optical region can meet the resolution and other requirements. Optical rangefinders may be active or passive, that is, they may direct a beam of energy to the target or use a natural source such as sunlight, and they may utilize a number of different principles which include time-delay measurements, triangulation, interferometry, and optical effects such as focusing and parallax in various guises. Several of these approaches are discussed in a report by Biernson, Euling, and Jarnagin.[3] The weight, power, and sunlight constraints imposed strongly favor an active rangefinder utilizing a laser, with a semiconductor injection laser being a particularly attractive choice because of its small size and weight and its compatibility with miniaturized electronics. The strictures on moving parts coupled with the necessity to scan a significant area militate against the use of triangulation or focusing techniques; thus the sensor con-

Received December 12, 1970; revision received June 28, 1971. This paper presents the results of one phase of research performed at the Jet Propulsion Laboratory, California Institute of Technology, sponsored by the NASA under contract NAS 7-100. The author wishes to express his thanks to A. Johnston, J. Moore, and S. Saunders for many helpful discussions.

Index category: Extraterrestrial Surface Transportation.

* Associate Professor of Electrical Engineering.

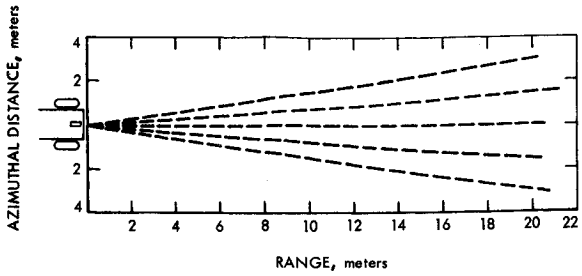

Fig. 1 Azimuthal beam paths for laser diode array.

figuration which appears to be best adapted to the requirements of the Mars Rover application is one utilizing an injection laser in the pulse time-delay measurement or radar mode. With the choice of rangefinder type made, the obstacle detector design divides into three major areas: the rangefinder design, choice of scan configuration and design of the scan mechanism, and the devising of methods of interpreting the information obtained by the rangefinder.

Scan Requirements and Mechanisms

An upper bound to the range at which the rangefinder should operate is determined by the geometry of the situation. If it is assumed that the sensor is located at a height of 2 m above the surface of the terrain, then at ranges much greater than about 20 m even gentle surface undulations would serve to mask pits and depressions entirely and would make it difficult to unambiguously discern the presence of a positive obstacle such as a boulder. Assume that it is desirable to scan an area extending from a few m distant out to 20 or 30 m. This requires only a small scan angle if the vehicle attitude and terrain surface are level, but a considerable increase in scan angle is necessary to compensate for more realistic angles between vehicle attitude and the mean surface in front of the vehicle.

A reasonable azimuthal scan requirement is that the observed area be at least as wide as the swath of the roving vehicle at useful elevation scan positions. A wider azimuthal scan would be desirable if large numbers of obstacles were expected, but since this is not the case, alternate vehicle headings can be explored simply by steering the vehicle.

Achieving the desired scan without the luxury of moving parts poses a difficult problem indeed. A large variety of electro-acoustic, electrooptic, and piezoelectric beam deflection techniques exist,[4,5] but none are capable of achieving large scan angles without considerable complexity and perhaps not at all with the multimode output characteristic of an injection laser. Additionally, these techniques are best adapted to beams of very small diameter, while both transmitted and received beam diameters must be on the order of tens of mm in this application. If no "moving" parts is interpreted to mean no wearing parts, a suitable elevation scan can be achieved by use of a resonant vibrating mirror of the fork or taut band type, and the much less stringent azimuth requirement can be met by use of a transmitting array. The specific scheme proposed employs an array of 5 laser diodes (operated one at a time), properly positioned along the focal plane of a convergent lens to give the azimuth pattern shown in Fig. 1, while the receiver beam is shaped into a fan pattern by use of a cylindrical lens and not scanned in azimuth. Only one of the lasers in the array is operated during each elevation scan, so 5 elevation scans are required to completely scan the pattern. As Fig. 1 shows, the use of only 5 laser diodes at the particular spacing chosen is marginal in that the azimuthal beamwidth does equal the vehicle width (assumed to be 2 m) at ranges greater than 7 m, but the azimuthal resolution is better than 0.5 m only for ranges less than about 7 m. This situation is considerably alleviated by the fact that a particular portion of a scene will be scanned many times from slightly different aspects as the vehicle progresses.

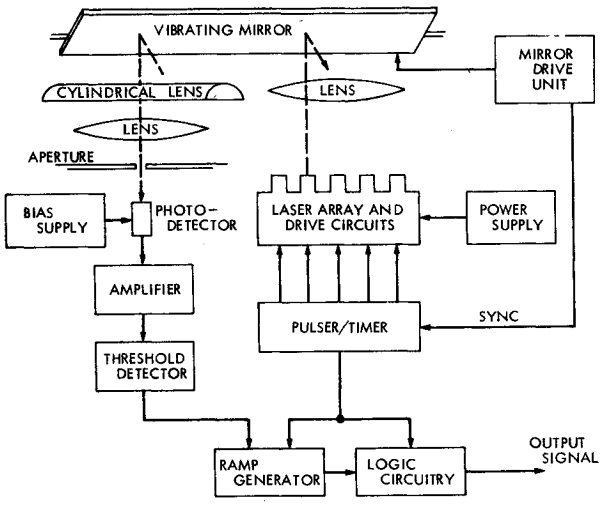

Fig. 2 Block diagram of the proposed sensor.

A specification for a suitable vibrating mirror includes a 25 Hz vibration frequency, ±12.5° peak mirror excursion (50° total beam deflection), and a 30 mm by 60 mm mirror size, with the long axis parallel to the axis of rotation. This size mirror permits the transmitter and receiver beams to be side by side; it might also be possible to use 2 separate vibrating mirrors if they can be synchronized sufficiently closely. The elevation scan is sinusoidal, but can be partially linearized by utilizing only a portion of the mirror excursion. If the mirror attitude is set so that its equilibrium position is looking down from the horizontal by 0.15 rad (8.6°) and its usable scan angle is ±0.25 rad (±14°), then it will scan a range from 5 m out to infinity when the vehicle attitude and surface are level, from 3 m out to about 13 m when the vehicle-mean surface angle is −0.25 rad, and from 13 m out to infinity when the vehicle-surface angle is +0.25 rad. Since the vehicle-surface angle should be even this large for only brief periods, this range of scan angle appears to be adequate.

The beam swept out by the vertical scan moves at an angular rate of 68.5 rad/sec in the vicinity of the mirror equilibrium point, so a transmitter pulse repetition rate of 10 kHz means that the terrain is sampled at 0.61 m intervals at the midrange distance of 13.3 m for the level vehicle attitude-level terrain case. The geometry of the situation automatically results in finer resolution being attained at closer ranges—the samples are spaced at approximately 6 cm at a range of 4 m—and less fine resolution at greater ranges, an eminently sensible arrangement. Since only one laser diode is operated on each vertical scan, the entire field is scanned once each 0.2 sec, a time which is sufficiently short that vehicle pitching and rolling should only occasionally interfere with a scan. At the nominal condition of level vehicle attitude and level terrain, a vehicle traveling at a velocity of 0.139 m/sec (0.5 km/hr) will detect a given obstacle 900 times in the 5 to 30 m search range. This redundancy will be somewhat reduced by vehicle pitching, but is still of such a magnitude as to suggest spending some of it in combatting false alarms; that is, requiring that an obstacle be sensed several times in succession before the sensor signals the presence of an obstacle.

Rangefinder Design

The next topic considered is the design of the rangefinder used in the sensor. Major components of the sensor are shown in block diagram form in Fig. 2. The transmitter portion of the proposed rangefinder consists of an array of 5 gallium-arsenide laser diodes, each equipped with its own driving circuitry. Each laser diode has a typical output of 13 w from an emitting area on the order of 3 by 225 μm. The diffraction-limited beamspread for the smaller laser dimension is on the order of 0.3 rad, and it is desired to illuminate the target

area with a beam of the smallest possible diameter in order to minimize target-induced pulse spreading and split returns, thus a collimating lens is necessary. It is difficult to predict precisely the effect of a spherical lens on the laser beam since it is multimode and not circularly symmetric, but a 25 mm f/3.2 simple lens should collect at least 80% of the radiation emitted by any one of the five diodes and project it onto a spot never larger than 0.1 m in diameter for ranges up to 30 m. The diodes must be spaced at 6 mm intervals along the lens focal plane in order to achieve the scan coverage of Fig. 1. The function of the pulser/timer is to sequentially operate one laser of the array on each elevation sweep and to fire the laser diodes at a 10 kHz rate and with a pulse duration of about 4 nsec.

The receiver portion of the proposed rangefinder consists of collecting optics, photodetector, amplifier, and threshold detector. The receiver optics consists of a 25-mm diameter simple lens followed by a cylindrical lens to produce a receiver beamwidth of 3 mrad in elevation and 0.4 rad in azimuth. This particular beamshape includes in its field of view all the azimuthal area which can be illuminated by the transmitter, but is otherwise as small as possible in order to reduce the amount of background solar radiation intercepted. The receiver optical system also contains a 50 Å optical filter to further discriminate against background radiation, where the optical bandwidth is as narrow as laser characteristics permit. Room temperature gallium-arsenide injection lasers emit at a nominal wavelength of 9020 Å, with an output wavelength-spread on the order of Å (caused by multimoding and by heating within the duration of a pulse). There are differences between diodes on the order of tens of Å because of material and processing variations, and the output wavelength shifts with diode temperature at a rate of approximately 1.75 Å/°C; thus a 50 Å optical bandwidth is a compromise between obtaining good background rejection and requiring tight wavelength control. The choice of postdetection bandwidth is dictated by the requirement of maintaining a sufficiently fast rise-time to preserve the pulse leading edge, and the bandwidth requirement in turn places an upper bound on the allowable load resistance. The value of solar spectral irradiance is determined from quantities given in Allen,[6] while the value for Martian surface reflectivity is from Meisenholder.[7] The receiver antenna area is selected to be small but comparable to the area required for the transmitter optics, and all other parameter values are dictated by characteristics of available components. Sensor performance is calculated for 3 different types of detectors—silicon PIN photodiode, avalanche photodiode, and photomultiplier tube—for the case that detection is based on a threshold criterion.

The signal power delivered to the detector's photocathode is

$$P_r = P_t\Gamma_t\Gamma_r\xi T_a A_r/2\pi R^2 = 0.1219 \times 10^{-3}/R^2 \quad (1)$$

which is 0.135 μw at a range of 30 m and 4.87 μw at a range of 5 m.

The solar background power at the detector photocathode is given by

$$P_b = M\alpha_v\alpha_h T_a B\xi\Gamma_r A_r \cos\Phi/2\pi \quad (2)$$

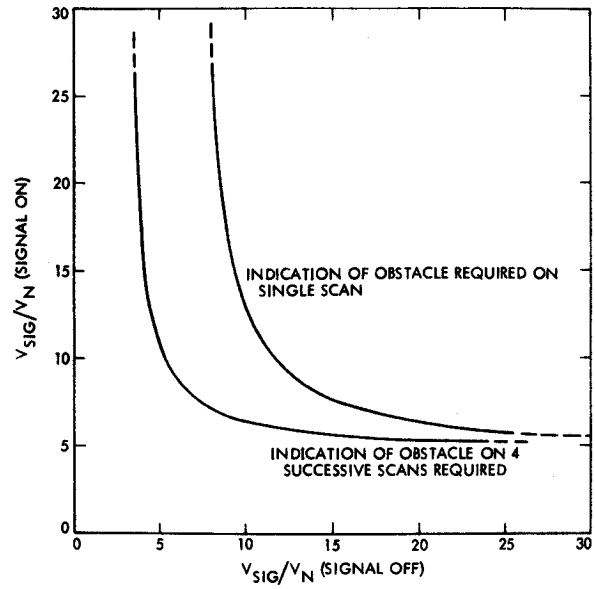

Fig. 3 Curves relating minimum signal-to-noise ratios.

and taking the worse-case situation of the sun directly overhead ($\Phi = 0$), P_b is found to be 0.028 μw and is independent of range.

If the photodetector is characterized by a quantum efficiency Q—we must use "fast" and "slow" values Q_s and Q_n for the case of an avalanche photodiode—and a dark current I_d, the mean value of current leaving the photocathode is

$$I_{av} = I_d + e\lambda(Q_s P_r + Q_n P_b)/hc \quad (3)$$

and the standard deviation is given by $(2e\Delta f I_{av})^{1/2}$. The distribution of photoelectrons is Poisson, but since there are many electrons per independent observation interval, the process is adequately modeled by Gaussian statistics. In the latter form the shot noise due to incident signal and background radiation and internal effects may be conveniently combined with the thermal nose of the detector load resistance and the noise contributed by a postdetection amplifier. If the preamp passband is set to pass the high frequencies associated with a fast pulse rise time but not the low frequency fluctuations induced by scanning terrain of varying albedo, etc., the rms noise voltage output of the preamp is

$$V_n = A_v[G^m R_L^2 2e\Delta f I_{av} + F4kT\Delta f R_L]^{1/2} \quad (4)$$

The mean value of preamp output voltage during a signal pulse is given by

$$V_{sig} = A_v R_L G Q_s e\lambda P_r/hc \quad (5)$$

and the voltage signal-to-noise ratio is obtained by combining the various equations as shown below

$$\frac{V_{sig}}{V_n} = \frac{\left(\frac{e\lambda}{hc}\right)R_L G Q_s P_r}{\left\{2e\Delta f G^m R_L^2\left[I_d + \frac{e\lambda}{hc}(Q_s P_r + Q_n P_b)\right] + 4kT\Delta f R_L F\right\}^{1/2}} \quad (6)$$

Table 1 Voltage signal-to-noise ratios at the post-dectector amplifier output for various types of detectors

	V_{sig} (20 m range) / V_n (signal off)	V_{sig} (20 m range) / V_n (signal on)	V_{isg} (30 m range) / V_n (signal off)	V_{sig} (30 m range) / V_n (signal on)
PIN photidiode	0.276	0.276	0.123	0.123
Photomultiplier	9.41	2.75	4.18	1.88
Avalanche photodiode with				
G = 20	3.29	3.24	1.46	1.45
G = 100	13.25	9.76	5.89	5.02
G = 200	17.05	10.34	7.58	5.71

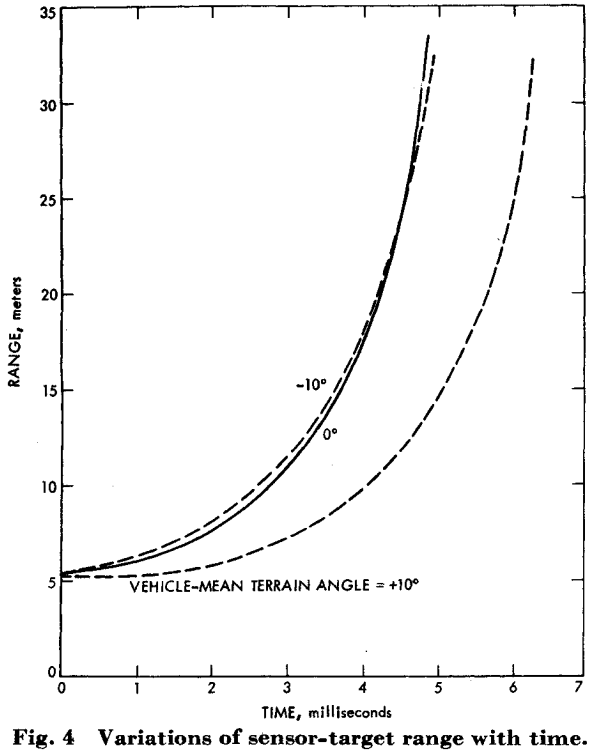

Fig. 4 Variations of sensor-target range with time.

Numerical values are summarized in Table 1 for ranges of 20 and 30 m for the worse-case situation of the sun directly overhead.

The dominant source of noise in the case of the PIN photodiode detector is thermal noise in the load resistance, and the results shown in Table 1 indicate that an increase of transmitted power or receiver antenna area of 2 orders of magnitude would be necessary in order to use this particular device (a signal-to-noise ratio of 10 is the approximate requirement). The photomultiplier's high internal gain makes load thermal noise negligible, but its low quantum efficiency and the relatively large value of background illumination limit its performance. The avalanche photodiode is a semiconductor with properties that fall between a silicon photodiode and a photomultiplier, but has two peculiarities which degrade its signal-to-noise performance somewhat. One is that all incident photons are not immediately absorbed, and as a result the device has a substantially lower value of ac compared to dc quantum efficiency. The other undesirable characteristic is that the avalanche internal gain mechanism is not noiseless; this is accounted for in the device model by the exponent of the gain being different for noise power than for signal power. This latter characteristic gives rise to an optimum value of gain which maximizes the signal-to-noise ratio for any particular set of circumstances. The optimum value of gain for the particular set of parameter values used in the calculations is beyond the typical attainable value of 200 but does not result in performance significantly better than that achieved with a gain of 200. The results given in Table 1 indicate that an avalanche photodiode operated at a gain on the order of 100 or 200 yields an adequate signal-to-noise ratio at a range of 20 m and a marginal one at 30 m; thus this is the device that would be incorporated into the sensor.

Table 2 Range differences in meters between successive pulses at several ranges and vehicle-tarrian angles for the proposed sensor operating on flat terrain

Nominal ground range, m	Vehicle-terrain angle = −10°	Vehicle-terrain angle = 0	Vehicle-terrain angle = +10°
5	0.090	0.077	0.035
10	0.327	0.359	0.289
20	1.178	1.394	1.300
30	2.558	3.192	2.964

For the case of signal detection based on a threshold criterion, the signal-to-noise ratio necessary in a particular application is determined by the need to set a threshold voltage level which is sufficiently high that it is only rarely exceeded by noise peaks in the absence of a pulse but not so high that it fails to detect signal pulses. To calculate the threshold level necessary to ensure that false alarms occur no more than, say, once a month, we observe that there are on the order of 60 signal pulses per line scan, 300 pulses per field, 1500 pulses per sec, and 2×10^9 pulses per month (assuming 12 hr of operation per day). From sampling theory, independent voltage samples occur every two nsec for a 250 MHz bandwidth. If range-gating is employed so that only times up to 200 nsec are considered (the time for a pulse to return from up to a 30 m range), there are 100 independent observation intervals per pulse, and on the average half of these would occur before receipt of a signal pulse. Thus a false alarm rate of one per month requires that the probability of the signal-absent noise exceeding the threshold be about 10^{-11}, however this number is not particularly critical because of the rapid exponential decline of the wings of Gaussian functions. If we define a missed pulse as one which is not detected in one observation interval of two nanoseconds, then the probability of a missed pulse is equal to the probability that the signal-present noise exceeds the difference between the mean signal level and the threshold voltage. The sensor might detect a given obstacle as many as 900 times as the vehicle progresses, and this calculation will result in a threshold which will be increasingly exceeded by the signal level as the range to the obstacle is reduced, so a reasonable requirement is that a missed pulse occur no oftener than once a minute. This requires that the probability of the signal-present noise exceeding the mean signal-threshold differences be about 10^{-5}. From tables of Gaussian probabilities, we can write

$$V_T \geq 6.71 V_n \text{ (signal off)}$$

and

$$V_{sig} - V_T \geq 4.26 V_n \text{ (signal on)} \qquad (7)$$

where V_T signifies the threshold voltage. Combining these equations yields an equation constraining possible values of signal-to-noise ratios.

$$\frac{6.71}{V_{sig}/V_n \text{ (signal off)}} + \frac{4.26}{V_{sig}/V_n \text{ (signal on)}} \leq 1 \qquad (8)$$

A similar analysis shows that the signal-to-noise requirements can be relaxed if it is required to sense the presence of an obstacle a number of times before triggering an output. If it

Table 3 Number of pulses necessary for the sensor to scan from bottom to top of 0.2 m and 0.5 m positive step obstacles at various ranges and vehicle-mean terrain angles

Nominal ground range L, meters	Angle between vehicle and mean terrain	Positive 0.2 m step at range L	Positive 0.5 m step at range L
5	+10°	15	37
	0°	7	17
	−10°	6	14
10	+10°	4	9
	0°	3	8
	−10°	4	8
20	+10°	2	4
	0°	2	4
	−10°	2	5
30	+10°	1	3
	0°	1	3
	−10°	2	4

Table 4 Range differences between successive pulses divided by range for 0.2 m and 0.5 m negative step obstacles for various ranges and vehicle-mean terrain angles

Nominal ground range L, m	Angle between vehicle and mean terrain	No obstacle	Negative 0.2-m step at range L	Negative 0.5-m step at range L
5	+10°	0.006	0.097	0.205
	0°	0.014	0.104	0.211
	−10°	0.017	0.106	0.213
10	+10°	0.028	0.117	0.223
	0°	0.034	0.122	0.227
	−10°	0.032	0.120	0.226
20	+10°	0.063	0.148	0.250
	0°	0.066	0.151	0.253
	−10°	0.057	0.143	0.246
30	+10°	0.095	0.177	0.276
	0°	0.098	0.180	0.279
	−10°	0.080	0.164	0.264

is required to detect an obstacle on four successive frames, the equation constraining possible values of signal-to-noise ratios becomes

$$\frac{2.91}{V_{sig}/V_n \text{ (signal off)}} + \frac{4.55}{V_{sig}/V_n \text{ (signal on)}} \leq 1 \qquad (9)$$

Equations (8) and (9) are plotted in Fig. 3. Note that the requirement of a multiple indication of an obstacle not only eases the performance requirements but also greatly reduces the probability of false alarms caused by anomalies not considered in this analysis.

The ranging accuracy of the proposed rangefinder is difficult to calculate, but can be estimated from experimental results on other systems. A laser profilometer reported by Hopson[8] uses the same type of threshold detection system considered here with about the same over-all pulse risetime; experimental results for that system indicate a range accuracy of ±10 cm.

Interpretation of Rangefinder Returns

The interpretation of returned signals to determine whether or not an obstacle is present can be accomplished in a variety of ways. One possible method is to use a fast timer to measure the elapsed time between the emission of a pulse and the detection of the return. This information is then fed to the vehicle computer along with vehicle attitude information. The angular coordinates of each pulse are known from timing considerations, so the computer can be programed to distinguish obstacles to any desired degree consistent with the sensor resolution. Another possible method, which would not require the use of the vehicle computer at all, is to convert each elevation scan into an analog waveform containing the desired information. If a fast ramp initiated when a pulse is transmitted is terminated upon receipt of a return signal or the passage of 200 nsec (the time for a signal to travel 30 m and return), whichever comes first, the range information will be preserved as a sequence of equally spaced pulses whose amplitudes are proportional to range. In the case of level terrain, the pulse train for each individual sweep would increase approximately quadratically in amplitude with time on a scale determined by the angle between vehicle and terrain. The presence of a positive obstacle, such as a boulder, would be manifested by a smaller than normal or even negative increase in amplitude between successive pulses, while a larger than expected increase would signal the presence of a negative obstacle such as a fresh crater. The technique of comparing each pulse's amplitude with that of its immediate predecessor ignores nearly all the information in the return but looks specifically for the most characteristic indication of an obstacle—the presence of a discontinuity in range as a line-of-sight is swept. Unfortunately, it does not appear feasible to detect obstacles on the basis of pulse-to-pulse differences only. As shown in Fig. 4, the angle between vehicle and mean terrain is a significant factor. The apparent asymmetry between the three curves of Fig. 4 is caused by the nonlinearity of the sinusoidal scan compensating the geometric range nonlinearity in one case and complementing it in the other. Range differences between successive pulses vary considerably, as summarized in Table 2 below. Values are tabulated for the level vehicle-level mean terrain case and for vehicle-mean terrain angles of ±10°.

Because of the geometry, positive (step up) and negative (step down) obstacles may best be discerned by different criteria, although in either case we assume that a 0.5-m step is an obstacle while a 0.2 m step is not. A distinctive feature of a positive obstacle is that the range increase is small or zero for several successive pulses, as the scan travels from the bottom of the obstacle to the top. The quantity $\Delta R/R^2$ is approximately constant for level terrain over a 5–30-m range for vehicle-mean terrain angles within ±10°; thus, one method of determining the presence of a positive obstacle is to count the number of pulses for which $\Delta R/R^2$ falls below a fixed threshold. The return of greater than some predetermined number of successive pulses (e.g., 3 or 4) for which $\Delta R/R^2$ was below threshold would signal an obstacle. As an indication of the sensitivity of this criterion, the number of successive pulses necessary for the sensor to "see" the top of positive 0.2 m and 0.5 m step obstacles is given in Table 3. The figures indicate that this particular criterion fails at the 5 m range because it cannot distinguish a 0.2 m step from a 0.5 m step over the complete range of vehicle-terrain angles, but can be used at greater ranges. The data of Table 3 also show that it would be desirable to make the number of pulses required to signal an obstacle dependent on the range.

On the other hand, it is suggested that the criterion for detection of a negative obstacle be the occurrence of a value of $\Delta R/R$ larger than a predetermined threshold. Table 4 below gives values of the range difference between successive pulses divided by the range, $\Delta R/R$, and indicates that this criterion is adequate to detect negative obstacles if the threshold is set at approximately 0.180. The use of the quantity $\Delta R/R$ rather than $\Delta R/R^2$ yields a criterion that is more independent of range and terrain angle.

Conclusions

The proposed sensor contains optical components that are relatively small, light, and few, and the electronic components are all of the miniature solid-state type; thus the weight of the overall sensor is primarily that of the mechanical packaging and should be 10 lb or less. If a power efficiency of 0.1% is assumed for the laser diodes, a pulse duration of four nsec, and a pulse repetition rate of 10 kHz half of the time (no transmission during vibrating-mirror scan retrace), the power required by the laser diodes is about 0.26 w. The vibrating mirror drive power is on the order of 10 mw; thus the total power requirements should be only a few watts. It appears entirely feasible to discern the presence of obstacles by use of relatively simple processing.

References

[1] *Mars Surface Models (1968)*, NASA SP-8020, May 1969.

[2] Moore, J. W., "Surface Navigation on Mars," paper presented at the National Space Meeting of the Institute of Navigation, Moffett Field, Calif., Feb. 1970.

[3] Biernson, G. A., Euling, R., and Jarnagin, W. S., "Range Sensor Techniques for Automatic Object Identification," AFCRL-69-0503, Nov. 1969, Air Force Cambridge Research Labs., Bedford, Mass.

[4] Fowler, V. J. and Schlafer, J., "A Survey of Laser Beam Deflection Techniques," *Proceedings of the IEEE*, Vol. 54, Oct. 1966, pp. 1437–1444.
[5] Kulcke, W., Kosanke, K., Max, E., Habegger, M. A., Harris, T. J., and Fleisher, H., "Digital Light Deflectors," *Proceedings of the IEEE*, Vol. 54, Oct. 1966, pp. 1419–1429.
[6] Allen, C. W., *Astrophysical Quantities*, University of London, Athlone Press, 1955, pp. 140 and 155.
[7] Meisenholder, G. W., "Planet Illuminance," TR 32-361, Nov. 1962, Jet Propulsion Lab., California Inst. of Technology, Pasadena, Calif.
[8] Hopson, J. E., "Low Altitude Laser Measurement System," AFFDL-TR-67-176, Dec. 1967, Air Force Flight Dynamics Lab., Wright-Patterson Air Force Base, Ohio.

OCTOBER 1971 J. SPACECRAFT VOL. 8, NO. 10

Plasma Generator for Space Vehicle Neutralization

H. J. KING* AND SEIJI KAMI†
Hughes Research Laboratories, Malibu, Calif.

An experiment was conducted in which pulses of high velocity electrons were ejected from a space probe flying a ballistic trajectory. To maintain the electrical neutrality of the vehicle during the experiment, a plasma generator of the MPD arc type was used to create a trail of charged particles which, in turn, provided a conductive path between the vehicle and the ambient space plasma. The plasma generator system consists of a modified Penning type discharge, power conditioning system, argon reservoir, and valve. The total package, 12 in. × 6 in. diam, weighs 9.6 lb and is capable of generating a net positive ion current of greater than 1 A with a power input of less than 200 w.

I. Introduction

THE basic function of the plasma generator is to maintain vehicle electrical neutrality during periods when the onboard experiment emits 50 kv, 0.1 A electron pulses. If neutrality were not maintained during such pulses, the vehicle would charge rapidly to a high positive potential and the electron beam would be either degraded in energy or returned to the vehicle.

The system requirements are that the plasma generator emit a minimum of 0.1 A positive ion current at a positive bias voltage of less than 50 v with respect to the vehicle. The flight duration is less than 10 min.

II. Basic Operation

The device, which resembles the low power MPD arc thruster,[1] consists of a cylindrical anode with a coaxial cathode immersed in an axial magnetic field, as shown in Fig. 1. In operation, the majority of the electrons emitted thermionically from the cathode are confined by the magnetic field to axial cycloidal motion; thus they can reach the anode only by collisions with neutral atoms, ions, or other electrons. The theory of this ionization and conduction mechanism has been discussed in detail by Bowditch,[1] Domitz,[2] and Meyerand.[3]

The basic concept which emerges from these descriptions is that a plasma is formed in the discharge chamber and the plasma potential is approximately equal to anode potential. Downstream of the source the plasma potential falls rapidly as a result of the divergent magnetic field and the decrease in neutral density shown in Fig. 1. The electrons are thus contained electrostatically at the ends of the discharge chamber and oscillate axially back and forth in a manner similar to that of a low-voltage Penning discharge. Ions are accelerated by an axial electric field caused by the electric pressure gradient which exists in the region of diverging magnetic field.[1] The downstream voltage is self-adjusting to permit just enough high-energy electrons to escape to equal the ion current and hence maintain charge neutrality if the source is electrically isolated from its surroundings. If the source is electrically biased with respect to the surroundings, the net current flow may be controlled. In this way the specification that the source must emit 0.1 A at a maximum bias of 50 v can be met. As will be shown below, the source readily emits this quantity of current at zero bias.

The relatively short time available between the start of the program and the freezing of a flight design limited the experimental investigations to those parameters necessary to assure that the basic specifications could be met and that a satisfactory control system could be implemented. Argon was used successfully as the expellant in all tests, although other gases or vapors would undoubtedly serve as well.

III. Laboratory Performance Tests

The experimental circuit is shown in Fig. 1. With this arrangement the beam current (the positive ion current leaving the engine) was recorded by an ammeter in the bias line as a function of the neutral gas flow to the plasma gun for different discharge currents. This was done for engine bias voltage of 0, +6, and +12 v. During these experiments the axial magnetic field was kept constant at 25 g (because the performance is relatively insensitive to the magnetic field as long as the field is above a critical value ≈ 15 g). All test data reported here were taken using the breadboarded flight supplies which incorporate a feedback loop to maintain a preset value of discharge current by adjustment of the filament heating power. In addition to the instrumentation shown in Fig. 1, there was a beam scanning Faraday cup which could be moved axially and rotated through 360°.

Presented as Paper 69-273 at the AIAA 7th Electric Propulsion Conference, Williamsburg, Va., March 3–5, 1969; submitted December 18, 1970; revision received July 22, 1971. The authors wish to acknowledge the many valuable discussions and assistance of J. Winckler and R. McEntire of the Univ. of Minnesota during the course of the project.
Index category: Electric and Advanced Space Propulsion; Sounding Rocket System; and Spacecraft Propulsion System Integration.
* Head, Propulsion Technology Section. Associate Fellow AIAA.
† Staff Engineer. Member AIAA.